780434

Design Considerations in Energy Absorption by Structural Collapse

C. L. Magee and P. H. Thornton
Research Staff, Ford Motor Co.
Dearborn, MI

ABSTRACT

A general treatment of the absorption of mechanical energy by the axial collapse of a variety of structural shapes, including tubes, honeycombs and foams is developed which encompasses both the geometry of the structure and also the material properties. The use of the method in the design of load bearing structures in which energy absorption is an additional design function is illustrated. High strength-to-weight ratio materials offer a significant weight saving for energy absorbing components, although such materials may have a reduced tensile ductility. The implications to situations in vehicle crashworthiness are discussed.

ALTHOUGH THE THEME of this paper, the absorption of kinetic energy by structural collapse, is concerned in particular with energy absorption in an automobile structure, the principles to be discussed will be applicable to all situations involving energy absorption. Historically, the automobile structure has been fabricated almost exclusively from mild steel over the entire period in which automobiles have been built, so that a wealth of experience has accumulated with regard to the behavior of the basic material and of the structure itself in a wide variety of loading conditions. In consequence, the mechanical response of mild steel has tended to be taken for granted, particularly in those design aspects which involve forming, joining and notch sensitivity for example. A new set of boundary conditions for the design of automobile structures has evolved recently with respect to weight reduction and damageability which has necessitated serious consideration of materials other than the traditional construction material. This transition has highlighted the fact that the tests and empiricisms which have proved satisfactory in the past for the design of structures using mild steel become inadequate at best and misleading at worst, with these newer materials.

Materials have been ranked conventionally in terms of mechanical strength parameters derived from tensile, impact and hardness measurements. Other quantities, such as fracture toughness and fatigue strength are more difficult to determine and since they are primarily of interest in more specialized areas, they will not be considered further in this report. The conventional mechanical properties and design methods have permitted the production of successful designs which can operate under load bearing circumstances because the maximum stresses involved in the structure are kept below the failure limit of the material, i.e., the structure in all parts remains in an elastically stressed condition. However, in structural collapse, the material comprising the structure is

0148-7191/78/0227-0434$02.50

undergoing failure either by extensive plastic deformation, usually at relatively high rates, or even by fracture while the structure is simultaneously performing its design function. Structural analysis methods are not yet capable of handling these complexities. Our approach is to identify experimentally those material and geometric characteristics which are relevant to this situation of structural collapse and which can easily be determined. We are then able to derive empirical but quantitative expressions which are useful in design and materials selection.

Within the framework of design for energy absorption and weight reduction, there are three key parameters which will be considered further. The most important, the specific energy, is the ratio of the maximum energy that can be dissipated to the specimen weight. For an ideal absorber it is related to the mean collapse load P_m by the relation

$$E_s^c = \frac{\int P dx}{Vp} = \frac{P_m}{A_s \rho} \qquad (1)$$

where V is the volume, A_s is the area and ρ is the density. The second parameter is the collapse efficiency which is a measure of how much of the structure is available to absorb the energy. As described below, collapse efficiencies can be defined on either a geometric, load or energy absorbing basis and are attempts to measure the efficiency with which the structure uses the available space in dissipating or storing the kinetic energy of a moving object. The third parameter, the operating stress, is the stress level at which the energy dissipator functions and is defined as

$$\sigma_N = \frac{P_m}{A_o} \qquad (2)$$

This is an important quantity because P_m is related to energy and deceleration while A_o represents the area needing protection.

THE MATERIALS AND STRUCTURAL DEPENDENCE OF THE SPECIFIC ENERGY ABSORPTION

SPECIFIC TENSILE ENERGY ABSORPTION - The specific tensile energy absorption, E_s^T, is a parameter which is readily determined from a tensile test by measuring the area under the load-elongation curve. The strength level and the uniform elongation (extension to the peak load) play a combined role in determining this energy absorbing capacity, so that factors which affect these quantities, e.g., heat-treatment condition, will have a marked influence upon the specific tensile energy absorption. It has been shown (1)* that E_s^T can be related to the ultimate tensile strength σ_u and the uniform true strain ε_u by the expression

$$E_s^T = \frac{\sigma_u \varepsilon_u}{\rho(1 + \varepsilon_u)} \qquad (3)$$

where ρ is the density. A comparison of values derived from Equation 1 with experimentally determined values for a variety of materials (1,2) is shown in Table I and it is seen that Equation (3) is quite adequate for predicting E_s^T if σ_u and ε_u are known. To maximize E_s^T, both a high σ_u and ε_u are required. Cold worked steels which have combinations of high σ_u and low ε_u will have a low tensile energy absorption, whereas metastable austenitic stainless steels, which have combinations of high σ_u and ε_u show a superior tensile energy absorption.

STRUCTURAL SPECIFIC ENERGY ABSORPTION - The previous section described how materials could be ranked by their specific tensile energy absorption in terms derived from the standard tensile test. However, when materials are incorporated into a structure, extra complexities arise because the geometry of the structure has now been introduced as a variable and, in addition, the primary load on the structure may no longer be tensile in nature. The classical criteria by which failure of a structure is avoided are based upon maximum elastic deformation or upon very small plastic deformation, e.g., high-strain fatigue criteria. When a structure is successfully absorbing energy, the material is usually undergoing extensive plastic strain. Failure of the material does not necessarily lead to failure of the structure for its design purpose, since the structure can continue to absorb energy to its limit provided that the failure zone remains relatively localized. Figure 1 shows tube samples of two aluminum alloys after such a collapse process; the 6061 alloy tube collapsed completely by buckling whereas the 2024 alloy tube disintegrated by longitudinal tearing. As shown in Figure 2, the collapse in both cases occurred under a fairly level, albeit fluctuating, load until the section had flattened completely. Furthermore, the resistance of the structure to continuing deformation can be affected by the geometry of the structure. The resistance of plates, loaded along the edge in compression, to continued deformation, is well known.(3) As shown previously (1) criteria based upon simple tensile tests for the ranking of specific energy absorption levels can be mis-

*Numbers in parentheses designate References at end of paper.

TABLE I

Specific Energy Absorbed in Tension; Comparison of Measured Values and Those Calculated from Equation 3

Material	σ_y GPa (ksi)	σ_u* GPa (ksi)	ε_u*	E_s^T kJ/kg (ft.lb./lb.) Measured	E_s^T kJ/kg (ft.lb./lb.) (Eq. 3)
4310 Steel (2)					
- Quenched from 1650°F (900°C)	NA	1.31 (189.6)	.0344	5.45 (1788)	5.56 (1824)
- Quenched					
- and Tempered at 600°F (316°C)	NA	1.21	.0257	3.82 (1255)	3.89 (1275)
- and Tempered at 1200°F (650°C)	NA	.7[illegible]	.0794	7.51 (2464)	7.43 (2440)
- Normalized (air cool from 1650°F (900°C)	NA	.782 (113.4)	.1297	11.5 (3759)	11.5 (3767)
- Austempered at 800°F (426°C)	NA	.848 (123.0)	.063	6.34 (2082)	6.44 (2109)
Corten A (as hot-rolled) (2)	.435 (63.1)	.693 (100.8)	.157	12.2 (3994)	12.1 (3961)
Corten B (as hot-rolled) (2)	.490 (71.0)	.687 (99.8)	.118	9.32 (3061)	9.30 (3047)
"Ultrasoft" (as received) (2)	.0771(11.2)	.276 (40.1)	.251	6.95 (2282)	7.11 (2328)
Normalized steels; compositions given in Ref. (2)					
Alloy A (low carbon iron)	NA	.347 (50.3)	.213	7.74 (2535)	7.80 (2558)
Alloy B	NA	.583 (84.7)	.196	1.23 (4041)	12.3 (4016)
Alloy C	NA	.862 (125.0)	.1266	1.22 (3988)	12.4 (4063)
Alloy D	NA	.535 (77.6)	.211	1.22 (4014)	11.9 (3910)

TABLE I (Continued)

Specific Energy Absorbed in Tension; Comparison of Measured Values and Those Calculated from Equation 3

Material	σ_Y GPa (ksi)	σ_u GPa (ksi)	ε_u*	E_s^T kJ/kg (ft.lb/lb) Measured	E_s^T kJ/kg (ft.lb/lb) (Eq. 3)
6061 Aluminum (1)					
Annealed	.0482 (7.0)	.137 (19.8)	.200	9.07 (2970)	8.75 (2,870)
Solution treated	.0628 (9.1)	.182 (26.4)	.217	12.4 (4070)	12.5 (4,097)
-T4	.124 (18.0)	.295 (42.8)	.200	18.5 (6060)	18.9 (6,190)
-T6	.277 (40.2)	.329 (47.8)	.0893	10.6 (3470)	10.4 (3,400)
1015 Steel (1)					
Normalized	.238 (34.6)	.419 (60.7)	.247	10.7 (3490)	10.3 (3,390)
Quenched	.495 (71.8)	.603 (87.5)	.063	4.46 (1465)	4.62 (1,513)

*As throughout these parameters are true stress and strain, for comparison to Reference (2) where engineering stress and strain were used, we can convert from σ^e_{ult} to σ_{ult} by the use of $\sigma_{ult} = \sigma^e_{ult}(1 + e_u)$ where e_u is the uniform engineering strain. Also ε_u the uniform true strain is obtained from $\varepsilon_u = \ln(1 + e_u)$.

leading when applied to structural components. In the case of structures, it is necessary to identify both the material and geometric contributions to the specific energy absorption. This will be done first for the most simple case, the axial collapse of cylindrical tubes, and the results will then be extended to the case of structures of more complex geometry.

Axial Collapse of Cylindrical Tubes - Materials Dependence -- It was shown previously (1) that materials properties play a significant role in the collapse of a structure. In order to ascertain this role it is necessary to remove the geometric dependence by examining the variation of E_s^c with constant geometry. This was done for cylindrical tubes of two t/D ratios and it was found (1,4) that over a wide range of materials conditions, a linear relationship existed between E_s^c and the specific ultimate tensile strength, σ_u^s, Figure 3. No

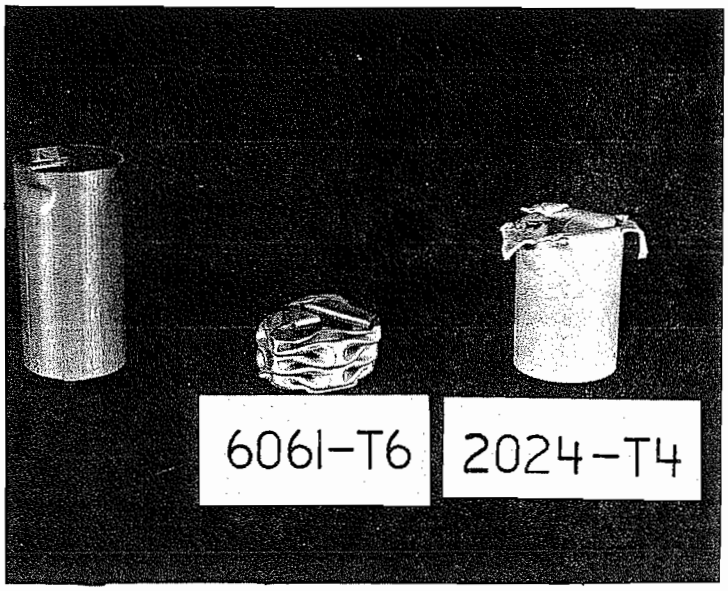

Fig. 1 - Samples of 6061 and 2024 aluminum alloy tube 1 in (2.54 cm) diameter after axial compression. The indentations to initiate the collapse process are shown in the uncompressed specimen

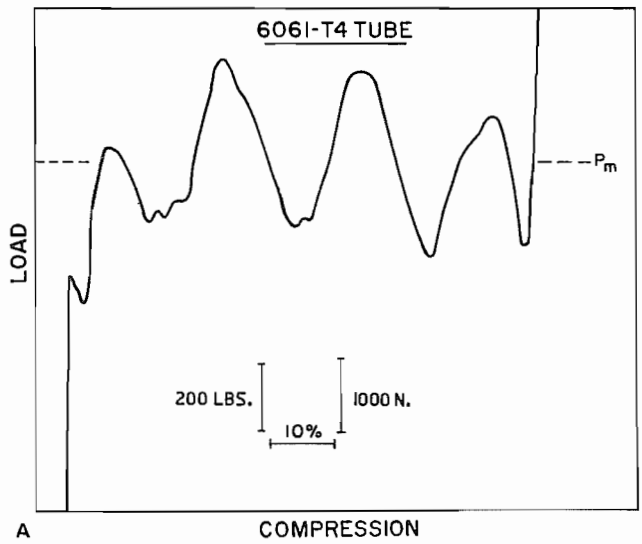

Fig. 2A - Load-deflection curve for a 6061-T4 aluminum alloy tube 1 in (2.54 cm) O.D. x 0.028 in (0.71 mm) wall

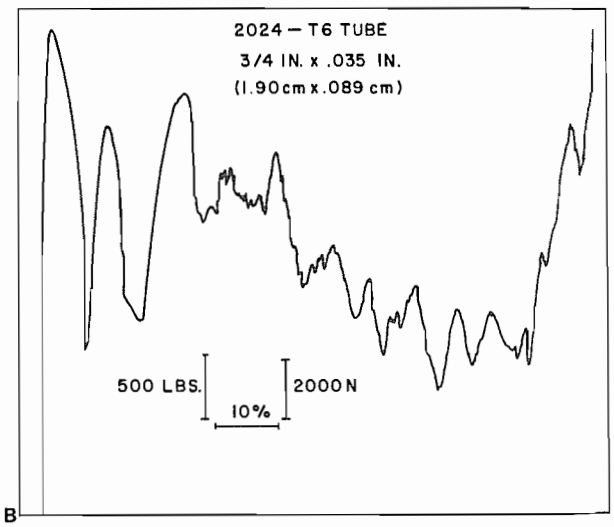

Fig. 2B - Load-deflection curve for a 2024-T6 aluminum alloy tube 3/4 in (1.90 cm) O.D. x 0.035 in (0.79 mm) wall

other property derived from the standard tensile test gave such a good correlation. The geometric instability which governs E_s^T does not affect the collapse process in an axially compressed tube, because the folding and stretching which accompanies the propagating buckle is accomplished while the collapse load is essentially constant throughout the collapse process. The good correlations of E_s^C with σ_u^S arises because the plastic strains produced in the material traversed by the propagating buckle are relatively large so that the work done during this process should be related to an average flow stress for large plastic strain.(1)

The correlation is not expected to be valid for cases where the material is brittle, when E_s^C might be expected to be less than values predicted from a simple proportionality to σ_u^S. However, some materials

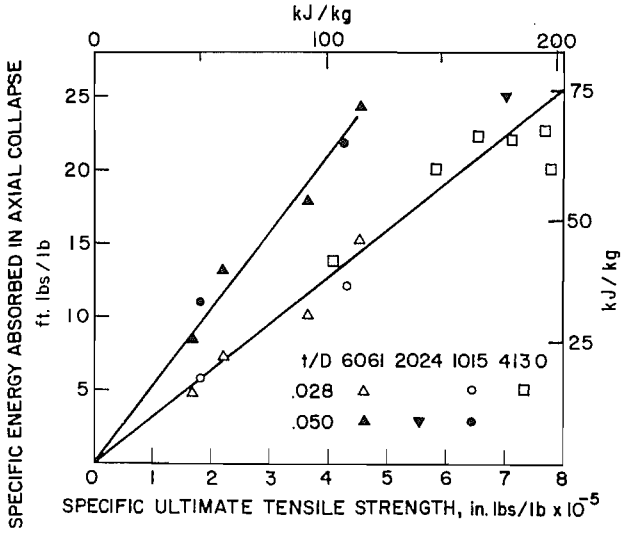

Fig. 3 - Comparison of the specific energy absorption in compression E_s^c and the specific tensile strength for a range of steel and aluminum alloys

shown in Figure 3 are of rather limited ductility, so that, over a fairly wide range of materials, σ_u^s is a good indicator of the ability of a material to absorb energy in a collapsing tube.

Structural Dependence - Structures of a given weight and made from the same materials are not necessarily equally effective in their resistance to deformation. Since at a fixed geometry, the energy absorbing capacity increases linearly with specific ultimate strength, Figure 3, a parameter (structural effectiveness) η can be defined by the expression

$$\eta = E_s^c/\sigma_u^s \quad . \qquad (4)$$

Then in this way the contribution of the material to the specific energy absorption can be eliminated and that of the geometric factor alone can be assessed. Figure 4 shows the variation of η with structural density ϕ* for cylindrical tubes of various materials. This data, derived from various sources in the literature (1,5-9), shows that η can be related to ϕ by the expression

$$\eta = 2\phi^{0.7} \qquad (5)$$

This expression is valid for tubes of any material provided that buckling is the prime mode of collapse. If structural collapse by a disintegration process occurs then the structural effectiveness is less.

* Structural density $\phi = \frac{\text{volume of material}}{\text{vol. encl. by structure}}$ and is equal to 4t/D for cylinders (see Table II).

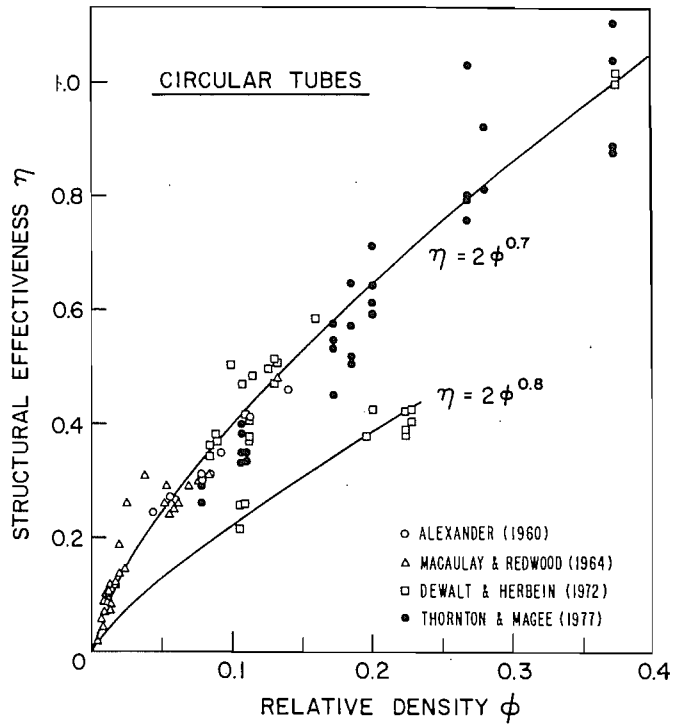

Fig. 4 - Variation of the structural effectiveness with structural density for cylindrical tubes in axial compression

As shown in Figure 4, for tubes of 2000 series aluminum alloys,

$$\eta = 2\phi^{0.8}$$

Figure 1 shows a partially collapsed 2024 aluminum alloy tube, where failure occurred partly by longitudinally propagating fractures.

This concept of structural effectiveness now provides a simple but effectual means to incorporate the geometric factor in the design of an energy absorber, since the complexity, if any, of the geometry in the structure is now reduced to a simply determined ratio. This ratio derived from data in references 4, 7-14, is shown for structures of increasing complexity in Figures 5-7 inclusive, for square (and rectangular) section tubes, honeycombs and foams respectively, and is summarized in Table II.

Edge-loaded flat plates are weaker than edge-loaded curved shells and so the structural effectiveness of square-section tubes, Figure 5, is less than that for cylindrical tubes. Honeycombs, Figure 6, are structurally highly effective because of their mutually supported elements. The efficiency of the structural effectiveness concept is particularly apparent in the case of foams, which are structurally very complex. Figure 7 encompasses the results of foams which display a very wide range of material charac-

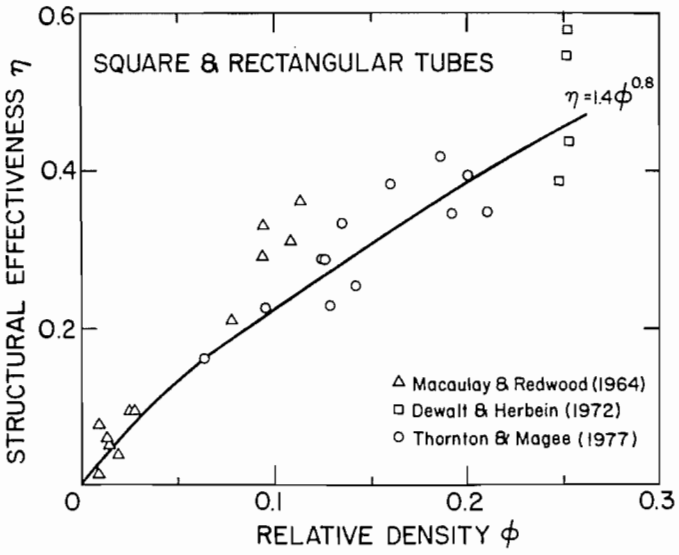

Fig. 5 - Variation of the structural effectiveness with structural density for square tubes in axial compression

teristics. If the matrix is able to undergo some plastic deformation, then $\eta \to 4\phi$, whereas if the matrix tends to be completely brittle, so that the foam disintegrates completely upon compression, then $\eta \to 0.8\phi$. The polyurethane foams, which are so useful commercially because of the ease with which their characteristics can be tailored for use, have a η value which falls between these two limits. For a given material, the structural effectiveness appears to be lower in the foam structure than it is in the tube form, probably because structural collapse occurs more by fracture rather than by bending. Also, foams show local variations in density; energy absorption is accomplished primarily by collapse (or fracture) of the thinner cell walls and the thicker nodes where the cell walls meet and which contain a large portion of the mass of the foam contribute very little toward the energy absorption capacity of the foam.

COLLAPSE EFFICIENCIES

Because of the nature of the buckling process, not all of the energy absorbing structure is usable; ultimately a point is reached where the structure has completely flattened and the load rises rapidly. Three measures of energy absorbing efficiency can be identified, as illustrated in Figure 8.

The geometric (or crush) efficiency is a measure of the packing of the folds during collapse and is given by the ratio of the actual compression to the original length, i.e.

$$e_G = \frac{\delta_c}{\ell_o} \qquad (6)$$

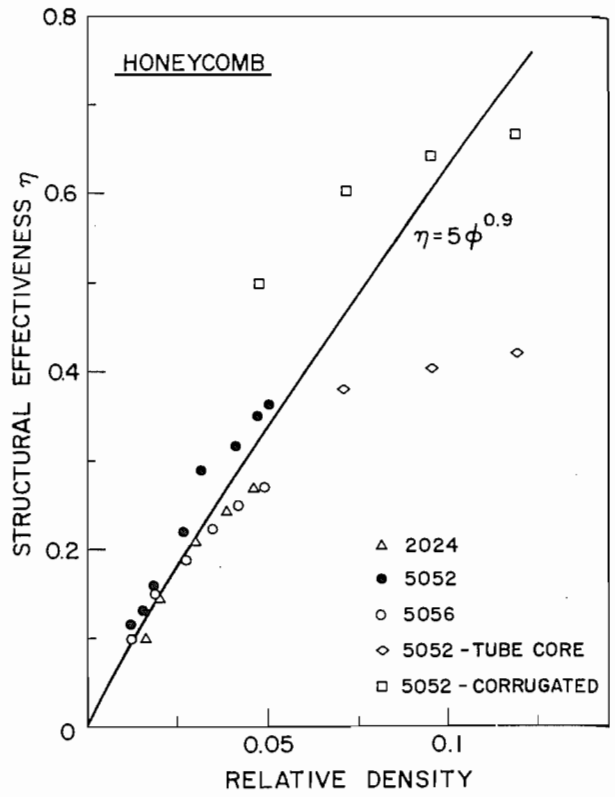

Fig. 6 - Variation of the structural effectiveness with structural density for honeycomb structures in axial compression

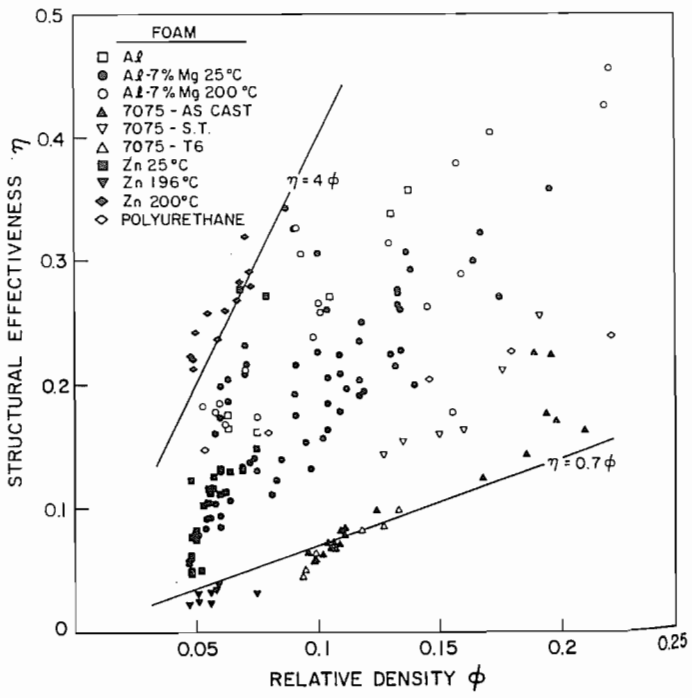

Fig. 7 - Variation of the structural effectiveness with structural density for foams in compression

TABLE II

Empirical Relationships between η and ϕ for the Collapse of Various Structures

Structure	$\eta = f(\phi)$	ϕ^*
Cylindrical tubes	$2\phi^{0.7}$	$4t/D$
Square and rectangular tubes	$1.4\phi^{0.8}$	$4t/S$
Honeycomb	$5\phi^{0.9}$	$8t/3S$
Foam	$0.7\phi - 4\phi$	ρ_f/ρ_m

* t = wall thickness; D = outside diameter; S = length of side; ρ_f = foam density; ρ_m = matrix density

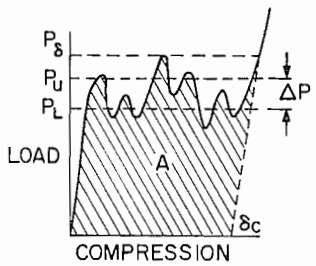

LOAD EFFICIENCY

$$e_L = 1 - \frac{\Delta P}{2P_u}$$

GEOMETRIC EFFICIENCY

$$e_G = \frac{\delta_c}{\ell_o}$$

ENERGY EFFICIENCY

$$e_E = \frac{A}{P_\delta \cdot \ell_o}$$

Fig. 8 - Geometric efficiency, load efficiency, and energy efficiency as a function of the collapse parameters

A second measure of efficiency is related to the load fluctuations which occur during the collapse. The load efficiency can be defined by

$$e_L = \frac{P_m}{P_u} \qquad (7)$$

where P_m is the mean collapse load and P_u is the mean of the upper collapse loads. If P_l is the mean of the lower collapse loads then e_L can be written

$$e_L = 1 - \frac{\Delta P}{2P_u} \qquad (8)$$

where $\Delta P = P_u - P_l$.

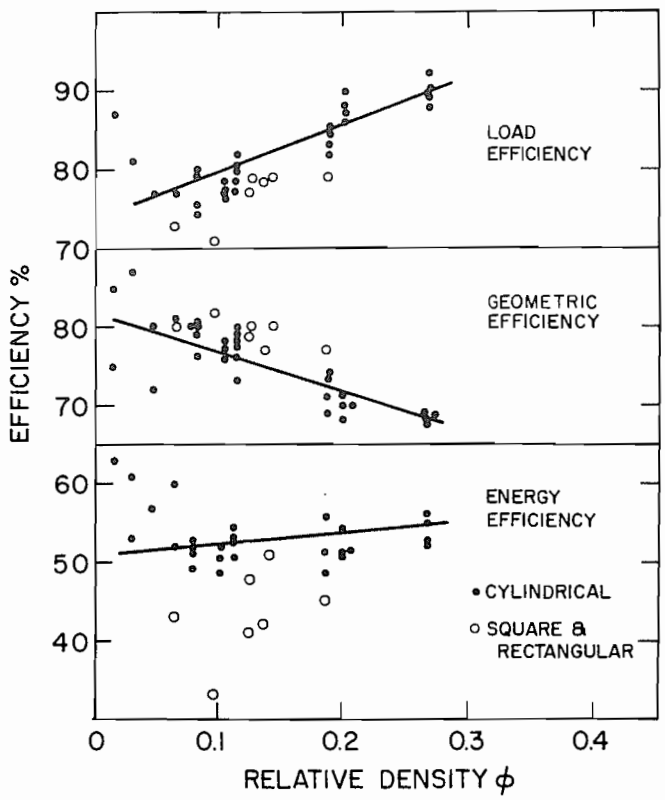

Fig. 9 - Geometric, load and energy efficiencies of energy absorption

The energy efficiency is related to the actual energy absorbed, given by the area A under the force-deflection curve, and is defined by

$$e_E = \frac{A}{P_\delta \ell_o} \sim \frac{P_m \delta_c}{P_\delta \ell_o} \qquad (9)$$

This quantity is the most difficult to measure but is the most rigorous representation since it combines all energy absorption efficiency factors. An ideal, "square-wave" energy absorber compresses at a constant force over its entire length, so that for the ideal case,

$$e_G^i = e_L^i = e_E^i = 1 \qquad (10)$$

The magnitude of these quantities will thus be affected by the magnitude and number of fluctuations in the load which occur during the collapse process. Hence the efficiencies will be functions of the structural density. As shown in Figure 9, the geometric efficiency, or crush efficiency decreases as the structural density increases, i.e. the folds do not pack together so closely with an increase in wall thickness for a given tube size. In contrast, the load efficiency tends to increase with increase in structural density, that is the load fluctuations become smaller relatively as the structural density increases. The energy efficiency, which is essentially the product of the load and structural efficiencies in consequence is practically independent of structural density. It must be remembered that e_E rises with increase in deformation, reaching a maximum at the point where the absorber has virtually completely collapsed and then falling rapidly with a continued increase in deformation. The values for e_E shown in Figure 9 represent the maximum values for each situation. It is seen that for practical energy absorbers e_E is approximately equal to (but slightly less than) the product $e_G e_L$.

A point brought out by Figure 9 is that discontinuities in section shape, e.g., corners, reduce e_E although increases in e_G may be observed. Flat sided structures pack better during collapse than do circular section structures, but the collapse of the relatively strong corners causes much larger fluctuations in the load. The independence of e_E with respect to ϕ is an important result with regard to the design of energy absorbers in different materials, as will be discussed further in Section V.

RATE EFFECTS

TENSION AND BENDING - The previous sections have underlined the observation that the specific energy absorption of a structure is a function of the ultimate tensile strength of the material rather than of any other mechanical strength parameter. For many materials, particularly structural steels, the mechanical properties depend upon the strain rate. In the case of structures which are absorbing energy at even moderate velocities, e.g. 5 mph (2.23 m/s) the strain rates are quite large in comparison to those employed in normal quasi-static testing. Davies and Magee (15) examined the tensile behavior at different strain rates of a range of engineering materials commonly used in structural applications and found that the tensile strength depended logarithmically upon the strain rate. The ratio of the high strain rate (5×10^4/min) tensile strength to that at the low strain rate (1/min) was greatest for hot rolled low carbon steel and diminished as the quasi-static tensile strength increased. No significant change in tensile ductility was found for any of the materials studied over the range of strain rates used.

In the collapse of structures, deformation rarely occurs by pure tension but by more complex modes which involve some element of bending. At any particular velocity, bending involves various strain rates since the outer and inner fiber strains differ. By studying materials behavior in four-point bending and in pre-bent hinge collapse, Davies and Magee (16) found that, for a similar variety of engineering materials as was used in their previous study (15), the dynamic factors for the loads in these more complex deformation modes were essentially the same as had been found for the tensile deformation, i.e. the materials were ranked in the same order with regard to their dynamic response independently of the evaluation procedure.

STRUCTURES - The collapse of structures has not been studied in so much detail as in the work described above, but sufficient work has been done to indicate that the deformation response is essentially the same as that of the material over a similar range of strain rates. It has been established (17) not only that the scaling laws (18) apply in the complex deformations which occur during structural collapse, a result which is of importance since it is often impracticable to perform a thorough experimental investigation on full-size structures, but also that simple cylindrical tubes have the same dynamic collapse response as complex, corrugated, rectangular section tubes (19).

To summarize, therefore, the variation of E_s^c for a structure with collapse rate will depend upon the collapse rate in the same manner as does σ_u. This gives a simple way of determining E_s^c for a structure since it can be tested under quasi-static condi-

tions and the strain rate correction established from the materials variation alone.

DESIGN OF ENERGY ABSORBING, LOAD BEARING STRUCTURES

The value of the relationships described above lies in that it is now possible to design a structure to fulfill an energy absorption requirement in addition to other structural load bearing requirements. It is first necessary to show how the average collapse load is related to the geometric and materials parameters described above. From the definition of specific energy, equation 1, the specific energy per unit length of ideal absorber is given by

$$E_s^c = P_m/\rho\ A_s \qquad (11)$$

where A_s = area of section and ρ = density.* Since $\sigma_u^s = \sigma_{u/\rho}$, then from Equation (4), the mean collapse load is given by

$$P_m = \eta\sigma_u A_s \qquad (12)$$

$$= \eta\sigma_u\phi\ A_o$$

where A_o is the overall area of the section as defined by its outer circumference.

In the design of energy absorbers which are made of different materials and which are also load bearing structures, rigidity, bending load and other loading situations must be considered in addition to energy absorption. Thus other sets of constraints exist which also must be met simultaneously. Examples will be given for the two cases of square section axial energy absorbers having either (i) equal rigidity or (ii) equal bending moment, at failure.

EQUAL BENDING RIGIDITY - In this section, the procedure will be outlined for the design of a centrally loaded beam which must also function as an axial energy absorber; the beam, in different materials, must have the same deflection under the central loading and must collapse axially under the same loads so as to absorb the same amounts of energy. Since frame rails can be required to meet rigidity and axial absorption criteria simultaneously, this example could be considered as a simple frame rail model.

* For the practical case of a real energy absorber (cf. Fig. 8) the specific energy is given by

$$E_s^c = \frac{P_m}{\rho A_s} \cdot e_G = \frac{P_\delta}{\rho A_s} \cdot e_E \qquad (11a)$$

From Table II, the relationship between the structural effectiveness and the structural density for a square section tube is

$$\eta = 1.4\phi^{0.8} \qquad (13)$$

If the tube has dimensions of S for the side and t for the wall thickness and assuming that S >> t, then from equations (12) and (13), the average collapse load for the tube will be given by

$$P_m = 17\ t^{1.8}\ S^{0.2}\ \sigma_u \qquad (14)$$

Note the small dependence upon S but the large variation with t. The moment of inertia is given by $I \sim tS^3/3$. Hence

$$I = \frac{1}{3}\left(\frac{P_m}{17}\right)^{15} \frac{1}{\sigma_u^{15}\ t^{26}} \qquad (15)$$

From equation (14), the tube dimensions for two materials to withstand a given collapse load will be given by

$$\frac{P_{m2}}{P_{m1}} = \left(\frac{t_2}{t_1}\right)^{1.8}\left(\frac{S_2}{S_1}\right)^{0.2}\frac{\sigma_{u2}}{\sigma_{u1}} \qquad (16)$$

Since equal collapse loads are required, $P_{m2}/P_{m1} = 1$. The flexure ψ of a centrally loaded beam must now be determined. For a given set of beam dimensions, $\psi \alpha 1/EI$. and because $P_{m2}=P_{m1}$, from equation (15) the ratio of the flexures will be

$$\frac{\psi_2}{\psi_1} = \frac{E_1}{E_2}\left(\frac{\sigma_{u2}}{\sigma_{u1}}\right)^{15}\left(\frac{t_2}{t_1}\right)^{26} \qquad (17)$$

Thus for tubes which are made of different materials having the mechanical properties shown in Table III and which have the same axial collapse load (i.e. the same energy absorption) and the same deflection under a given flexure load, equations (16) and (17) lead to relative tube dimensions and weight as shown in Table IV for a variety of common engineering materials. Note the significant weight reductions for these model frame rails with the higher strength-to-weight ratio materials.

The importance of the energy efficiency results shown in Figure 9 is now apparent. Table IV shows that considerable changes in section size result for axial energy absorbers constructed in alternative materials; the constancy of e_E with ϕ implies that the absorber will collapse with the same efficiency in each situation, i.e., that the average

Table III

Mechanical Properties of Materials

Material	U.T.S. ksi	U.T.S. MPa	E $lbs/in^2 \times 10^{-6}$	E GPa	σ_u^s $ft.lb/lb. \times 10^{-3}$	σ_u^s kJ/kg
Steel						
Mild Steel	55	379	30	207	16.0	47.8
950 HSLA	70	482	30	207	20.1	60.1
980 HSLA	100	689	30	207	28.7	95.9
Martensite*	170	1172	30	207	48.9	146
AISI 4340 (Quenched & Tempered)	240	1654	30	207	70.7	211
Aluminum Alloys						
5052-0	28	193	10	68.9	24.1	72.0
2036-T4	43	296	10	68.9	36.2	108
6061-T6	45	310	10	68.9	38.3	114
7075-T6	73	572	10	68.9	68.5	204
Plastic						
GFRP	10	68	2.5	17.2	10.4	31.1
GrFRP	200	1378	50	34.3	30.3	90.5

deceleration to which the moving object is subject will not be changed if energy absorbers made in different materials are used.

Although a weight reduction is observed with all of the alternative higher strength metals, this is obtained at the expense of an increase in the overall cross-section of the structure. Furthermore there are caveats which must be issued with respect to the results for the fiber-reinforced plastic beams and also for the dynamic values for the metal beams. Although E_s^c is directly proportional to σ_u^s over a wide range of tensile strength values, Figure 3, when the material becomes brittle, E_s^c, and hence η, starts to diminish. Current research has indicated that although the value of E_s^c for fiber reinforced plastic tubes is high, comparable to 6061-T6 aluminum alloy, it is less than would be expected from their high tensile strengths. Thus the weight reduction shown in Table IV for these materials may be too large. With regard to the dynamic values, there is little information available on the behavior of thin section structures fabricated from strong but relatively brittle materials. Also current research has indicated that structures made from moderately strong martensitic steel behave similarly to those made in mild steel; there is no information as yet regarding the behavior of structures made of high strength martensitic steels or of the high strength aluminum alloys.

EQUAL BENDING MOMENT - In this section, the procedure to design a beam which will withstand a given bending moment at failure and which has a given axial collapse load, will be outlined. This is an important case because members which are required to collapse axially are subject almost always to bending moments arising from, e.g., oblique impacts. If these bending moments are not resisted, then the member could develop an undesirable, unstable failure mode.

The stress moment M produced by bending is given by $M = \sigma I/C$, where C is the distance of the outermost fiber from the neutral axis. Hence, if $S >> t$, then from equations (14) and (15)

$$M = \frac{2}{3}\left(\frac{P_m}{17}\right)^{10} \frac{1}{\sigma_u^{\,9}\, t^{17}} \qquad (18)$$

If the tubes are proportioned so as to generate the same axial collapse load then the ratio of moments for two materials will be given by

$$\frac{M_2}{M_1} = \left(\frac{\sigma_{u1}}{\sigma_{u2}}\right)^9 \left(\frac{t_1}{t_2}\right)^{17} \qquad (19)$$

For tubes made of different materials, having the same axial collapse load and the same bending moment, equations (18) and (19) lead to relative tube dimensions and weights for various engineering materials as shown in Table V. Note that in this model, the high strength materials again can be very effective in reducing weight. However, the same caveats with regard to the behavior of the more brittle materials, as was discussed in the previous section, also are applicable here.

TABLE IV

Comparison of Dimensions and Weight for Square Tube Section Axial Energy Absorbers Having Equal Bending Rigidity Relative to a Mild Steel Structure

Material	Change % Quasi-Static (Dynamic)		
	Side	Thickness	Weight
Steel			
HSLA 950	+ 9(+ 7)	-22(-17)	-14(-11)
980	+16(+12)	-36(-29)	-25(-19)
AISI 4330 (Quenched & tempered)	+26(+20)	-50(-42)	-35(-31)
Aluminum Alloys			
5052-O	+34(+26)	+26(+50)	-43(-36)
2036-T4	+45(+37)	- 2(+17)	-51(-45)
6061-T6	+46(+38)	- 4(+14)	-52(-46)
7075-T6	+65(+55)	-33(-20)	-61(-56)
Composites*			
GFRP	+77	+126	+7
GrFRP	+12	-57	-91

* Calculated on basis of assumed specific tensile strength/specific energy absorption relationship.

TABLE V

Comparison of Dimensions and Weights for Square Tube Section Axial Energy Absorbers Having Equal Bending Resistance Relative to a Mild Steel Structure

Material	Change % Quasi-Static (Dynamic)		
	Side	Thickness	Weight
Steel			
HSLA 950	-10(- 8)	-21(-16)	-28(-21)
980	-17(-13)	-38(-27)	-44(-35)
AISI 4330 (Quenched & tempered)	-24(-20)	-47(-40)	-60(-52)
Aluminum Alloys			
5052-O	+12(+20)	+29(+51)	-51(-38)
2036-T4	+ 1(+ 9)	+ 2(+20)	-64(-55)
6061-T6	0 (+ 7)	0 (+17)	-66(-57)
7075-T6	-13(- 7)	-28(-15)	-78(-72)
Composites*			
GFRP	+42	+122	-12
GrFRP	-30	- 55	-94

* Calculated on basis of assumed specific tensile strength/specific energy absorption relationship.

EULER-RANKINE COLLAPSE - Rather than collapse in a progressive and stable manner, a tube can fail under compressive loading by Euler instability when the level of the compressive stress has reduced sufficiently the tangential modulus of elasticity. This alternative failure mechanism therefore must be avoided if an axial energy absorber is to perform its designed function.

The Euler-Rankine collapse load, P_{ER}, is given by

$$P_{ER} = \frac{\pi D t \sigma_u}{1 + \frac{\sigma_u}{\pi^2 E}\left(\frac{L}{D_m}\right)^2} \qquad (20)$$

where D_m is the mean tube diameter. When a tube is subject to axial collapse, as shown in Figure 2 the applied load fluctuates about the mean collapse load P_m so that the maximum load attained can exceed considerably the mean load. Thus in designing an axial energy absorber, a factor of safety should be included to ensure that the maximum load which will be encountered does not exceed the Euler-Rankine collapse load. In practice, it would appear adequate to make P_{ER} about 25% greater than P_m so that the correct collapse mode will always operate. Thus, putting $P_m \leq 0.8\ P_{ER}$ and using equations (5), (12) and (20), the material and geometric parameters for cylindrical tubes can be related by the expression

$$t/D \leq \left[\frac{0.152}{1 + \frac{\sigma_R}{\pi^2}\left(\frac{L}{D_m}\right)^2}\right]^{1.43} \qquad (21)$$

where σ_R is the normalized tensile strength given by σ_u/E. The critical relationship between t/D and L/D is shown in Figure 10 for several values of σ_R.* For a given σ_R, these curves show the maximum t/D ratio that is acceptable for a given L/D ratio. Tubes having a t/D ratio lying above the particular σ_R curve for that material, will undergo unstable collapse, while if the t/D ratio is below the σ_R curve, the tube will collapse in a progressive, stable manner.

The use of these equations will be illustrated by an example in which a tubular energy absorber was required to provide an average collapse load of 70,000 lbs. (312000N) under

* In Figure 10, the abscissa is plotted in terms of the tube outer diameter D rather than the mean diameter D_m for convenience in use.

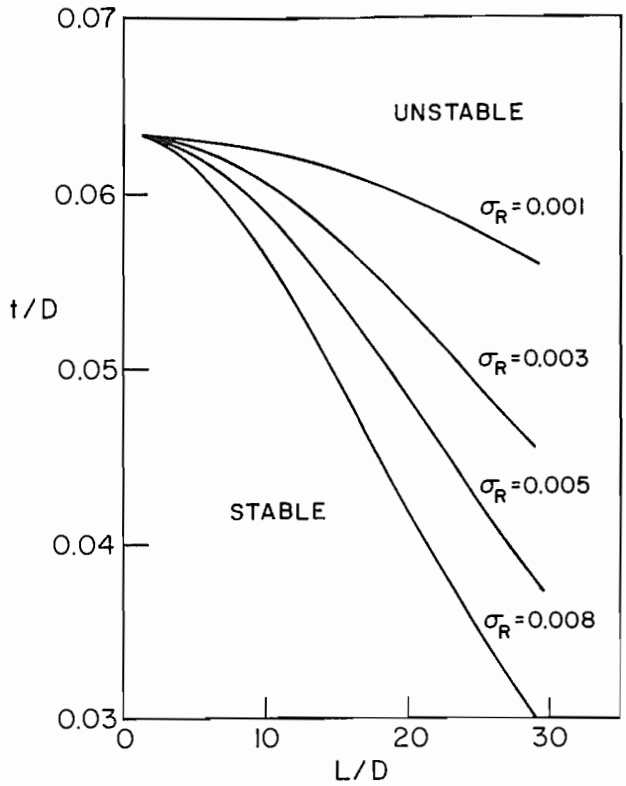

Fig. 10 - Relationship between geometric and material properties to prevent failure of a cylindrical tube by Euler-Rankine collapse

impact; the length of the tube was 28 in. (71.1 cm). Two mild steel tubes of different t/D ratios were prepared, which had approximately the required load characteristics. Three indentations were formed near one end to provide a trigger for the collapse process. The experimental results on the collapse of the tubes are shown in Section (1) of Table VI. The tube of smaller diameter collapsed in an unstable manner whereas the other tube collapsed in a stable manner. Section (3) of Table VI shows that the calculated P_{ER} for the larger tube is appreciably greater than the calculated (and observed) mean collapse load P_m, whereas the difference between P_{ER} and P_m was much less for the smaller diameter tube. The collapse response is reflected by the magnitudes of the critical and actual t/D ratios for the two tubes, as shown in Section (4) of Table VI.

Finally, Section (5) of Table VI gives values of P_{ER} (dynamic) for various sizes of tube, 28 in(71.1 cm) long, in both low carbon steel and HSLA steel, which have dynamic collapse loads P_m of 70,000 lb. (312000N), and also the proportion ΔP by which P_{ER} exceeds P_m. It is seen that for the low carbon steel tubes, the first size is unsatisfactory and the next larger is probably marginal, with respect to Euler-Rankine collapse. All of the HSLA tubes appear to be adequate. However, most important; it is found from this section that the 980 HSLA tubes will provide a 41% weight reduction for a given value of ΔP.

TABLE VI

Stable and Unstable Collapse in Steel Tube Energy Absorbers

(1) Experimental Results (Mild Steel)

Size	Average Collapse Load lbf. (N)	Peak Load lbf.(N)	Collapse Mode
2.5 in. X .17 in. (6.35 cm x .43 cm)	(unstable)	63500 (283000)	Euler-Rankine
3.0 in. X .18 in. (7.62 cm x .457 cm)	63500 (283000)	79500 (354000)	Tube folding

(2) Tensile Strengths (assumed)

	Quasi-static psi (GPa)	Dynamic psi (GPa)
Low carbon steel	50000 (.345)	60000 (.414)
980 HSLA steel	90000 (.676)	105000 (.725)

(3) Calculated quasi-static collapse loads (Mild Steel)

Size	P_{ER} lbf. (N)	P_m lbf. (N)	ΔP%
2.5 in. X .17 in. (6.35 cm X .43 cm)	60900 (271000)	53700 (239000)	13
3.0 in. X .18 in. (7.62 cm X .457 cm)	78300 (349000)	62400 (278000)	25

(4) t/D and L/D ratios

Size	σ_R	L/D	t/D	
			Actual	Critical
2.5 in. X .17 in. (6.35 cm. X .43 cm)	.00167	11.2	.068	.0605
3.0 in. X .18 in. (7.62 cm X .457 cm)	.00167	9.32	.060	.0615

(5) Comparison of low carbon and HSLA steel tubes for dynamic impact.

Steel	Size in. (cm)	P_{ER} lbf. (N)	ΔP%
Low carbon	2.5 X .179 (6.35 X .454)	76100 (339000)	9
	3.0 X .172 (7.62 x .434)	89900 (400000)	28
	3.5 X .168 (8.89 X .426)	104000 (463000)	49
HSLA 980	2.5 X .128 (6.35 X .325)	95400 (424000)	36
	3.0 X .124 (7.62 X .314)	114000 (506000)	63
	3.5 X .121 (8.89 X .307)	1317000 (585000)	88

FOAM REINFORCEMENT

One particular structural application of foams, and where some benefit has been claimed, has been in structural reinforcement. Selec-

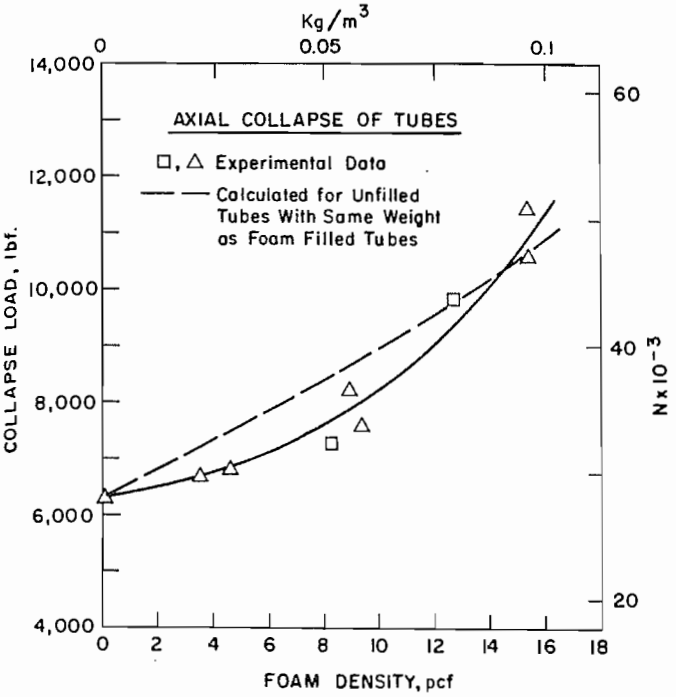

Fig. 11 - Axial collapse load of foam-filled 1010 steel tubes, 2 in (5.08 cm) O.D. x 0.35 in (0.89 mm) wall. For tubes of this size, it is more effective to increase the wall thickness than to foam-fill, if the density is below 14 pcf. (224 kg/m^3) (20)

tive foam filling was found to improve the crush characteristics of automobile bodies (19) and Davies and Magee (20) have investigated the effect of polyurethane foam filling upon the axial collapse load of 1010 steel tubes. As shown in Figure 11, foam filling was found to increase substantially the collapse load of the tubes, a 15 pcf. (240 Kg/m^3) foam for example producing approximately 70% increase in the collapse load. Similar increases were found for 6061 aluminum rectangular section tubes in bending. The strength of the insert was not the sole contributor to the load increase; bonding between the tube wall and the foam was necessary in order to attain the observed load increases, i.e. the foam increases the rigidity of the structure.

For foam filling to be effective, it must provide an increase in collapse load which is not attainable by other means. The collapse load can be raised by an increase in the wall thickness of the tubes. These loads also are shown in Figure 13 for thicker wall unfilled tubes having the same weight as the combined weight of the original section tube together with foam of various densities. It is seen that it is more weight effective to obtain the desired collapse load by an increase in the tube wall thickness if the foam has a density below 14 pcf. (224 Kg/m^3). Similar conclusions were reached for the case of

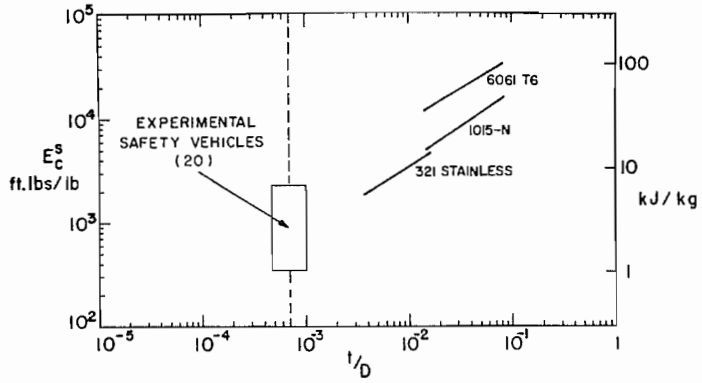

Fig. 12 - Specific energy of the automobile front-end structure relative to that of cylindrical tubes

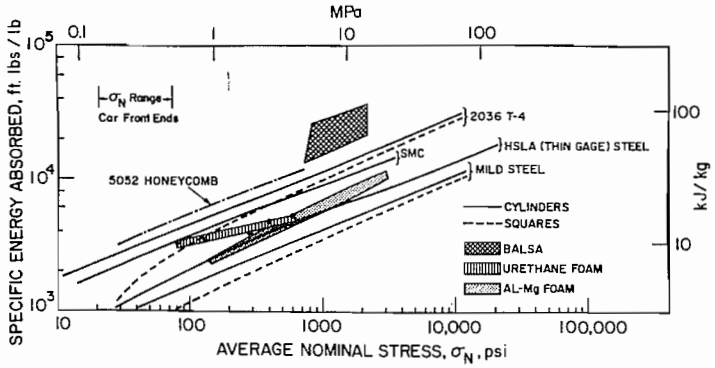

Fig. 13 - Relationship between specific energy and average nominal collapse stress for a variety of structures and materials

the foam filled beams. It was also observed that as the inherent strength of the tube structure decreases, then the initial foam density necessary for weight effectiveness also decreases.

Thus although large increases in collapse load may be obtained for a given section by foam reinforcement, the results should be carefully analyzed to see if the magnitude of the change is significant with respect to the cost and other penalties involved. This will be illustrated by means of results obtained from the crushing of a simple rectangular-section tube. The collapse loads (21) are shown in Table VII, where it is seen that a 94% increase in collapse load is achieved with a weight increase of only 17%. The problem is to determine if this change is weight effective.

A curved shell in edge loaded compression is a more rigid structure than is a flat plate similarly loaded. Thus any means used to increase the rigidity of a structure will be more effective in the case of a flat plate than for a curved shell. The disparity in

TABLE VII

Comparison of Foam Filling and Section Change on the Average Collapse Load of Rectangular and Cylindrical Low Carbon Steel Tubes

Section 4 in. X 2 in. X .083 in. (10.2 cm X 5.1 cm X .21 cm)+			
	Unfilled	Filled 12 PCF Foam (192 Kg/m^3)	Change %
Weight lbs. (Kg)	4.8 (2.2)	5.6 (2.5)	+17
P_m lb (N)	16000 (71200)	31000 (138000)	+94

Section	Average Collapse Load lbf. (N)	Weight Change %
2 in. X .065 in. (5.1 cm X .17 cm)	16000 (71200)*	-
2 in. X .083 in. (5.1 cm X .21 cm)	24000 (107000)*	+27
4 in. X 2 in. X .083 in. (10.2 cm X 5.1 cm X .21 cm)	16000 (71200)	+60
4 in. X 2 in. X .104 in. (10.2 cm X 5.1 cm X .264 cm)	31000 (138000)†	+27

+ Reference 21

* Reference 20

† Calculated

the collapse load for structures of different geometry caused by this rigidity difference is indicated in Table VII. Thus the weight effective density limit for a foam will be less for the rectangular section tube than it is for the cylindrical tube.

If it is assumed that the structural effectiveness of a rectangular section tube has the same relationship to the structural density as it does for a square section tube, then equations (13) and (14) can be used to calculate the collapse load of the rectangular sections. As shown in Table VII, in order to attain the same collapse load as the filled rectangular section, an unfilled section would have to have a wall thickness of 0.104 in. (2.64 mm), which would cause a weight increase of 27%. Thus the foam filling is weight effective in this case, but it should be noted that the weight increase due to the foam is only 10% less than that caused by the section thickness increase. The apparently significant changes produced by the foam filling are not really unattainable by other means and the foam filling may well not be cost effective in this application.

Situations in which foam filling is effective in causing an increase in the collapse load probably arise when collapse under stress in an unstable mode occurs, so that little energy is absorbed. By causing the structure to collapse in a more regular manner, and so to absorb a greater amount of energy, foam filling would be useful. This change of a structure from essentially a non-absorber to an absorber of energy could well be the most important role that foams play in improving the energy absorbing capability of a vehicle.

APPLICATION TO THE AUTOMOBILE STRUCTURE

The previous sections have given some indications of the factors involved in structural collapse and have described the interactions of materials variables, geometry, strain rate and scaling effects. Extending these concepts to the complexities of the automobile structure must necessarily involve some simplifications. Nonetheless, it is useful to examine our findings for possible relevance to the behavior of overall car structures. A first question that can be addressed concerns the order of magnitude that may be expected for specific energy absorption. We have seen that values for the specific energy absorption for simple tubes are of the order of 10^4-10^5 ft.lbs./lb. (30-300 kJ/kg). If one divides the energy absorbed in typical car barrier crashes by a reasonable fraction of the front end weight, one arrives at an estimated vehicle specific energy absorption in the range 10^2 to 3×10^3 ft.lb/lb. (.3-90 kJ/kg). These relatively low values for vehicles have sometimes been viewed as indicative of ineffectiveness, but Figure 12 demonstrates that they are, instead, consistent with the very low t/D ratio arising from the need to protect an entire vehicle front end rather than a point.

Although the E_s^c of structures made of HRLC steel and having $^t/_D$ ratios typical of those in automobiles have not been determined, stainless steel tubes having $^t/_D$ ratios nearly an order of magnitude lower than those of the 1015 steel tubes described earlier have been examined, and their E_s^c relationship with $^t/_D$ closely parallels that of the 1015 steel tubes, Figure 12. Thus an extrapolation by an order of magnitude from the results of the laboratory tests in order to derive values for E_s^c for an automobile does seem to be reasonable. Alternatively, this internal consistency indicates that the essentials can be understood by a study of relatively simple models.

An energy absorption parameter which now deserves further examination is the nominal collapse stress (load divided by area). In many vehicle design situations, the area which must be protected and the load (energy divided by crush length) are fixed input parameters. Thus if we compare the specific energy absorption capacity at equal collapse stress we will have a direct measure of weight effectiveness for different designs. A plot showing many of the approaches discussed herein is given in Figure 13. Very

few have been tested at the low nominal stresses that are of interest in real vehicles but with the extrapolation implied in Figures 12 and 13, one can conclude that (1) the ranking is similar to that drawn at higher nominal stresses; (2) foams (polyurethane and metal) are effective energy absorbers at their naturally low σ_N; this result is not obvious when absolute magnitudes of E_S^C are compared; (3) perhaps most importantly, these results indicate that significantly lighter weight structures can be achieved with higher strength steels and aluminum alloys. Indeed, this conclusion emerges strongly from all of the design examples reported here. This finding supports the crucial role of specific ultimate strength (1) in axial energy absorption. Of course, application of any of these conclusions awaits detailed design and prototype validation studies in complete vehicles.

REFERENCES:

1. P. H. Thornton and C. L. Magee, "The Interplay of Geometric and Materials Variables in Energy Absorption." J. Eng. Mat. Tech., Trans. ASME, vol. 99, 1977, pp. 114-120.
2. R. A. Grange, W. B. Seens and K. R. Phillips, "Effect of Microstructure on Energy Absorption of Carbon and Low-Alloy Steels in Uniaxial Tension." U.S. Steel Laboratories, Monroeville, Pa., 1970.
3. S. R. Timoshenko and J. M. Gere, "Theory of Elastic Stability", 2nd Ed., McGraw-Hill, New York, 1961.
4. P. H. Thornton and C. L. Magee, unpublished work.
5. Sir A. Pugsley and M. Macaulay, "The Large-Scale Crumpling of Thin Cylindrical Columns." Quart. J. Mech. Appl. Math., vol. 13, 1960, pp. 1-9.
6. J. M. Alexander, "An Approximate Analysis of the Collapse of Thin Cylindrical Shells Under Axial Loading." Quart. J. Mech. Appl. Math., vol. 13, 1960, pp. 10-15.
7. M. A. Macaulay and R. G. Redwood, "Small Scale Model Railway Coaches Under Impact." The Engineer, vol. 218, 1964, pp. 1041-1046.
8. R. C. VanKuren and J. E. Scott, "Energy Absorption of High-Strength Steel Tubes under Impact Crush Conditions", SAE 770213 presented at SAE Annual Meeting, Detroit, February 1977.
9. W. J. Dewalt and W. C. Herbein, "Energy Absorption by Compression of Aluminum Tubes", Report No. 12-72-23, Alcoa Research Laboratories, Alcoa Center, Pa., 1972.
10. "Mechanical Properties of Hexcel Honeycomb Materials", TSB120, Hexcel Corp., Dublin, California, 94566 (1971).
11. P. H. Thornton and C. L. Magee, "The Deformation of Aluminum Foams." Met. Trans., vol. 6A, 1975, pp. 1253-1263.
12. P. H. Thornton and C. L. Magee, "Deformation Characteristics of Zinc Foam". Met. Trans., vol. 6A, 1975, pp. 1801-1807.
13. E. A. Meinecke and R. C. Clark, "The Mechanical Properties of Polymeric Foams". Technonic, Westport, Conn., 1973.
14. T. K. Hill and W. W. Joseph, "Energy Absorbing Characteristics of Materials". Report No. SLA-74-0159, Sandia Laboratories, Albuquerque, N.M., 1974.
15. R. G. Davies and C. L. Magee, "Effect of Strain Rate Upon the Tensile Behavior of Materials." J. Eng. Mat. Tech., Trans. ASME, vol. 97, 1975, pp. 151-155.
16. R. G. Davies and C. L. Magee, "The Effect of Strain Rate Upon the Bending Behavior of Materials." J. Eng. Mat. Tech., Trans. ASME, vol. 99, 1977, pp. 47-51.
17. P. H. Thornton, "Static and Dynamic Collapse Characteristics of Scale Model Corrugated Tubular Sections". J. Eng. Mat. Tech., Trans. ASME, vol. 97, 1975, pp. 357-362.
18. H. L. Langhaar, "Dimensional Analysis and the Theory of Models". New York, N.Y., Wiley, 1951.
19. K. Brumm, "Report on the Third International Technical Conference on Experimental Safety Vehicles". Washington, D.C., 1972, Report No. DOT HS-820 217, pp. 2-194 - 2-197.
20. R. G. Davies and C. L. Magee, "The Effect of Foam Reinforcement on the Collapse of Beams and Tubes". Ford Scientific Research Staff, Technical Report No. SR-75-27, 1975.
21. J. A. Beckman, Parish Division, Dana Corporation, Taylor, Michigan, 1974.